JOURNAL OF MATERIALS SCIENCE 24 (1989) 4239–4245

Low thermal expansion and low thermal expansion anisotropy ceramic of $Sr_{0.5}Zr_2(PO_4)_3$ system

TOSHITAKA OTA, PING JIN, IWAO YAMAI
Ceramic Engineering Research Laboratory, Nagoya Institute of Technology, 10-6 Asahigaoka, Tajimi 507, Japan

A low thermal expansion ceramic with a very low thermal expansion anisotropy was synthesized from the $Sr_{0.5}Zr_2(PO_4)_3$ system. The sintering was promoted by addition of MgO, and the sol–gel technique also improved the sinterability. The thermal expansion of the crystal was lowered by substituting Nb^{5+} for Zr^{4+} and $1/2Sr^{2+}$ pairs, becoming near-zero for $Sr_{0.25}Nb_{0.5}Zr_{1.5}(PO_4)_3$. All dense ceramics in this system had a strength of about 80 MPa, and did not suffer microcracking even in the coarse-grained polycrystalline ceramics, owing to the very low thermal expansion anisotropy of the crystals.

1. Introduction

Some compounds in the $NaZr_2(PO_4)_3$ family have been reported to be low thermal expansion materials in recent years [1–8]. The crystal structure of $NaZr_2(PO_4)_3$ consists of a rigid three-dimensional network of PO_4 tetrahedra sharing corners with ZrO_6 octahedra and a three-dimensionally linked interstitial space occupied partially by Na^+ ions [6, 9, 10]. The total thermal expansion is influenced mainly by interstitial ions: for example, a smaller amount or a larger ionic radius of the interstitial ion results in a lower thermal expansion [6]. Therefore, for $KZr_2(PO_4)_3$ in which a larger K^+ ion was substituted for Na^+, or for $Na_{1-x}Nb_xZr_{2-x}(PO_4)_3$ which contained less interstitial ions, the total thermal expansion decreased and near-zero expansion ceramics were produced [7, 11]. However, when their ceramics were heated for long times at high temperatures, the grains grew to a large size and microcracking occurred because of the large thermal expansion anisotropy, resulting in a lowering of the strength. The critical grain size for microcracking is related to thermal expansion anisotropy, increasing when anisotropy decreases [12, 13].

The thermal expansion of $Sr_{0.5}Zr_2(PO_4)_3$ is relatively low ($\alpha_a = 2.6 \times 10^{-6}\,°C^{-1}$, $\alpha_c = 1.7 \times 10^{-6}\,°C^{-1}$ and $\alpha_{avg} = 2.3 \times 10^{-6}\,°C^{-1}$), and the thermal expansion anisotropy is very low [6]. Limaye *et al.* [8] reported the synthesis and expansion of $M_{0.5}Zr_2(PO_4)_3$ (M = Mg, Ca, Sr, Ba), but a dense ceramic of $Sr_{0.5}Zr_2(PO_4)_3$ has not yet been obtained. In this study, the synthesis of dense, strong and low thermal expansion ceramics with a very low thermal expansion anisotropy, which would remain free from a lowering of strength by microcracking, was attempted from the $Sr_{0.5}Zr_2(PO_4)_3$ system.

2. Experimental procedure

$Sr_{0.5}Zr_2(PO_4)_3$ was synthesized by the solid-state reaction and the sol–gel method. Starting materials were regent-grade chemicals. In the solid-state reaction method, $SrCO_3$, ZrO_2 and $(NH_4)_2HPO_4$ were wet-mixed in acetone, dried at 100° C, calcined at 300° C for 24 h, 600° C for 4 h and 900° C for 2 h, ground, and then fired at 1300° C for 24 to 48 h to obtain a single phase. The obtained powder was further ground to $< 2\,\mu m$. In the sol–gel method, $SrCO_3$ was dissolved in a 0.5 M aqueous solution $ZrOCl_2 \cdot 8H_2O$; then 0.5 M aqueous solution $(NH_4)_2HPO_4$ slowly was added to the solution with stirring. The reaction mixture was dried at 100° C and calcined at elevated temperature. $Sr_{0.5(1-x)}Nb_xZr_{2-x}(PO_4)_3$ solid solution was synthesized by the solid-state reaction of $SrCO_3$, ZrO_2, $(NH_4)_2HPO_4$ and Nb_2O_5.

The products were identified by X-ray powder diffraction, and the lattice parameters up to 1200° C were determined by high-temperature diffraction technique. Platinum powder was used as an internal standard. The diffraction patterns were measured in a 2θ range of 18° to 55° (Cu$K\alpha$) and up to ten major peaks were indexed.

After 0 to 5 wt % MgO was added as a sintering aid, test specimens for sintering were formed under 50 MPa in the shape of 16 mm diameter tablet or 5 mm × 5 mm × 60 mm bar, and then were sintered at temperatures ranging from 1100 to 1500° C. The bulk density of the sintered ceramics was determined by the Archimedean method using distilled water as a displacement liquid. The thermal expansion of the polycrystalline ceramics was measured from room temperature to 800° C with a silica glass differential dilatometer. The strength was measured by the three-point bending test. The microstructures were observed by a scanning electron microscope. Details of the above had been similar to those reported early [6, 7, 11].

3. Results and discussion

3.1. Synthesis of $Sr_{0.5}Zr_2(PO_4)_3$ ceramic

3.1.1. Solid-state reaction method

First, $Sr_{0.5}Zr_2(PO_4)_3$ powder prepared by the solid-state reaction was sintered. Dense polycrystalline ceramic

0022–2461/89 $03.00 + .12

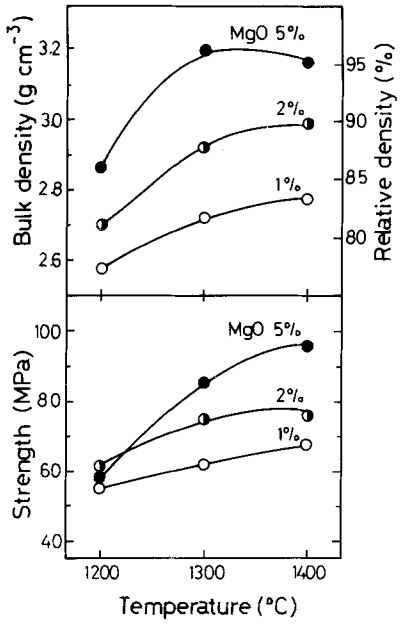

Figure 1 Variation of density and strength of $Sr_{0.5}Zr_2(PO_4)_3$ with sintering temperature and MgO concentration.

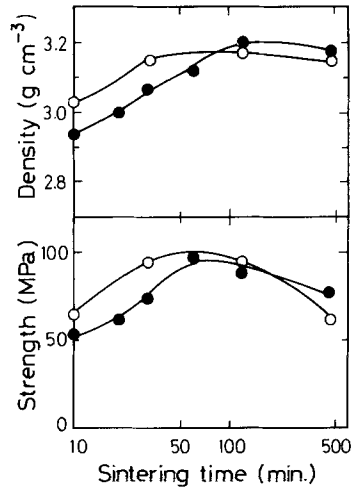

Figure 2 Variation of density and strength of $Sr_{0.5}Zr_2(PO_4)_3$ with sintering time.

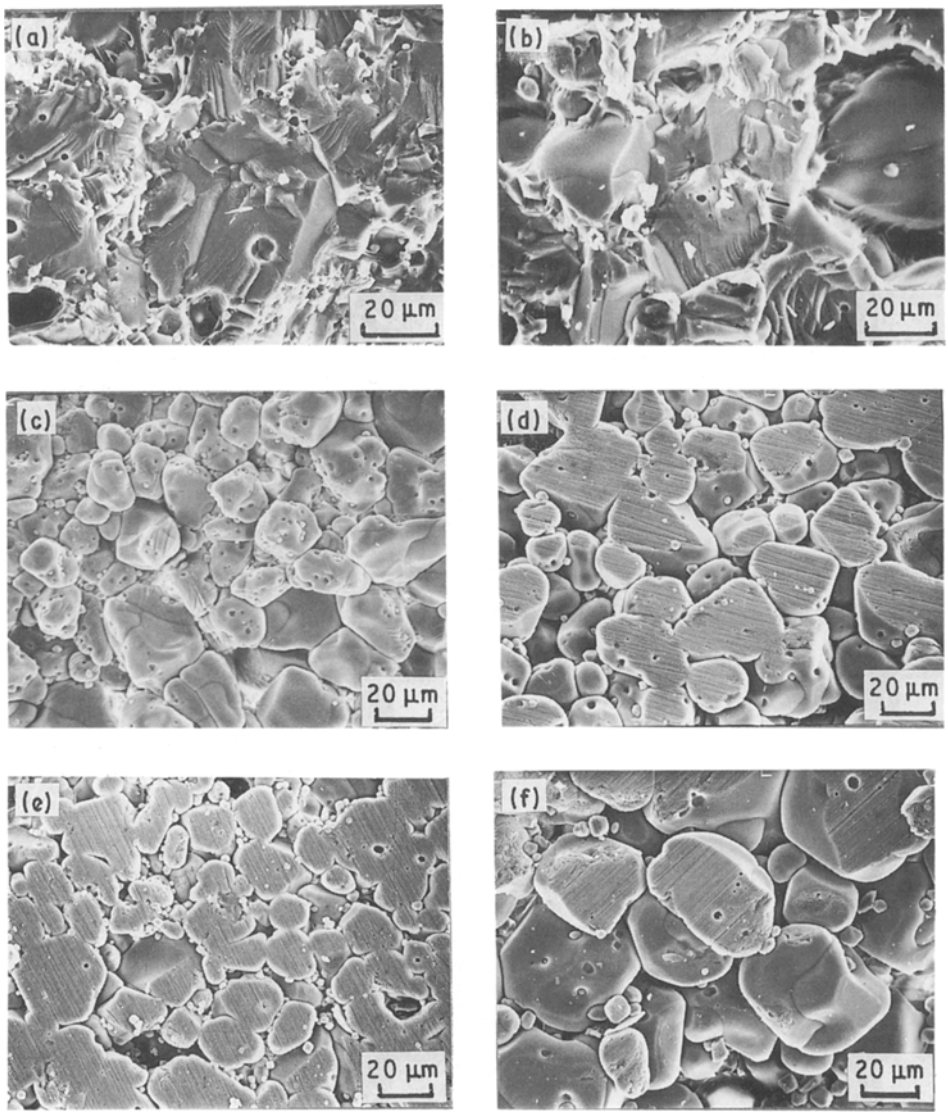

Figure 3 Scanning electron micrographs of fracture surfaces of $Sr_{0.5}Zr_2(PO_4)_3$ sintered with 5 wt % MgO: (a), (c) 1300° C for 1 h, (b), (f) 1400° C for 8 h, (d) 1300° C for 8 h, and (e) 1400° C for 1 h. (c) to (f) After etching.

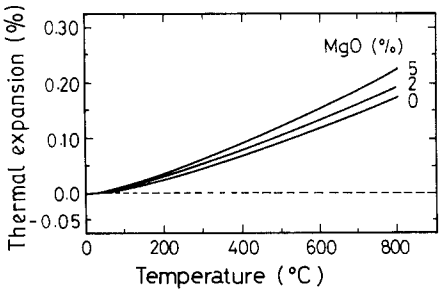

Figure 4 Thermal expansion curves of $Sr_{0.5}Zr_2(PO_4)_3$ ceramics.

could not be obtained by firing pure $Sr_{0.5}Zr_2(PO_4)_3$ even at $\geqslant 1500°C$. Accordingly, some MgO, which had been proved to be an effective sintering aid for the densification of $(ZrO)_2P_2O_7$ [14], $KZr_2(PO_4)_3$ [11] and $Na_{1-x}Nb_xZr_{2-x}(PO_4)_3$ [7], was added in order to obtain a dense and strong ceramic. Fig. 1 shows the variation of density and strength with sintering temperature and MgO concentration. Relative density up to 95% was achieved by sintering with 5 wt % MgO at $\geqslant 1300°C$. The densification rate of $Sr_{0.5}Zr_2(PO_4)_3$ was slow compared to $KZr_2(PO_4)_3$ and $Na_{1-x}Nb_xZr_{2-x}(PO_4)_3$, in which dense ceramics could be sintered with 5 wt % MgO at 1200° C in a short time. It was deduced that the predominant mechanism for densification of the $NaZr_2(PO_4)_3$ family was the sintering in the presence of a liquid phase such as an alkali phosphate [7, 11]. The minimum temperature of the liquid phase in the system $MgO–SrO–P_2O_5$ is higher than those of the systems $MgO–K_2O–P_2O_5$ and $MgO–Na_2O–P_2O_5$ [15]. In other words, an alkali metal such as sodium or potassium would decrease the melting point of the liquid phase formed during sintering. Therefore, it was believed that the densification of systems containing an alkali metal was accelerated at lower temperatures.

Fig. 2 shows the variation of density and strength with sintering time. The densification was almost completed by sintering for 2 h at 1300° C and for 30 min at 1400° C, and then the strength also increased with densification. Although the strength decreased a little after prolonged sintering, this decrease was obviously different from $(ZrO)_2P_2O_7$ [14], $KZr_2(PO_4)_3$ [11] and $Na_{1-x}Nb_xZr_{2-x}(PO_4)_3$ [7] in which the strength decreased drastically due to microcracking.

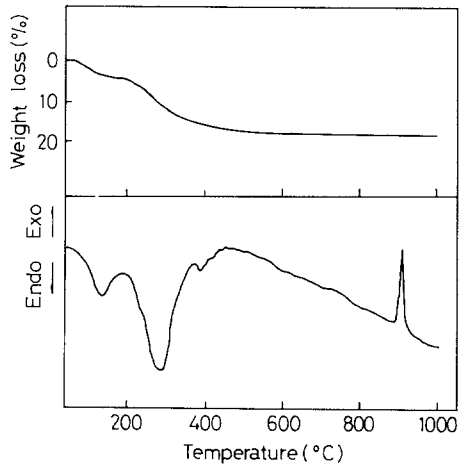

Figure 5 TG and DTA curves of $Sr_{0.5}Zr_2(PO_4)_3$ gel.

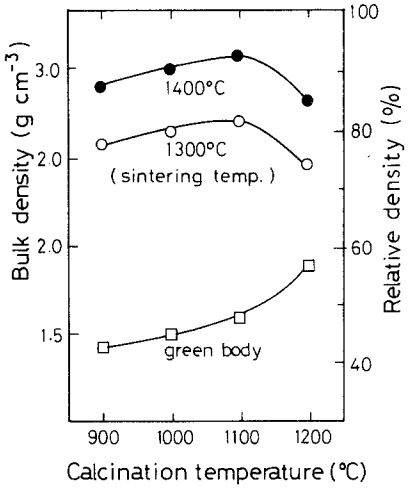

Figure 6 Influence of calcination on green density and sintered density of $Sr_{0.5}Zr_2(PO_4)_3$.

Fig. 3 shows the typical microstructures of the polycrystalline ceramics. As shown in Figs 3a and b, the fracture surfaces of dense samples presented uniform microstructures with some pores, which seemed to consist of a glass phase. The pore size became larger with increasing sintering time. When the surface was etched by HF solution, as shown in Figs 3c to f, grains appeared clearly. The grain size increased with increasing temperature and time, and reached $> 50\,\mu m$ at 1400° C after 8 h. However, no microcracks could be found even in coarse-grained ceramics. Therefore, it was concluded that the slight decrease in strength as shown in Fig. 2 was caused by only the effect of grain size.

Fig. 4 shows the typical thermal expansion curves of sintered ceramics. Not all the samples exhibited thermal expansion hysteresis loops, indicating that there were no microcracks in the polycrystalline ceramics. The ceramics of pure $Sr_{0.5}Zr_2(PO_4)_3$ without MgO had a linear thermal expansion coefficient of $2.1 \times 10^{-6}\,°C^{-1}$, which is near the average thermal expansion coefficient of the crystal. The thermal expansion coefficient increased with increasing amount of MgO, and reached about $2.9 \times 10^{-6}\,°C^{-1}$ for the sample sintered with 5 wt % MgO. It was considered that this increase of thermal expansion coefficient was due to the glass phase. Therefore, in order to decrease the amount of MgO as far as possible, a reactive fine powder was prepared by the sol–gel method.

3.1.2. Sol–gel method

Fig. 5 shows the TG and DTA curves of $Sr_{0.5}Zr_2(PO_4)_3$ powder prepared by reacting $SrCO_3$, $ZrOCl_2 \cdot 8H_2O$ and $(NH_4)_2HPO_4$ in an aqueous solution. The endothermic peaks and weight loss below 500° C corresponded to dehydration and release of other volatiles. The weight loss was slight at > 500° C. A sharp exothermic peak was observed at around 900° C in the DTA curve. The powder remained amorphous when calcined up to 800° C, and the XRD pattern of $Sr_{0.5}Zr_2(PO_4)_3$ single phase appeared at 900° C. Therefore, it was thought that the exothermic peak was the crystallization of the gel. In this method, a $Sr_{0.5}Zr_2(PO_4)_3$ single phase was formed directly from

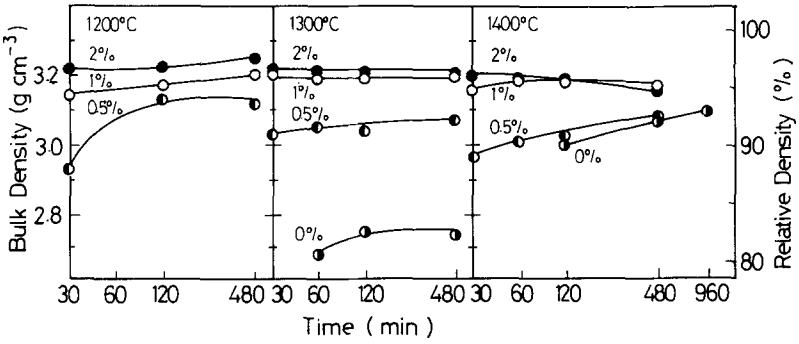

Figure 7 Variation of density with sintering temperature, time and MgO concentration.

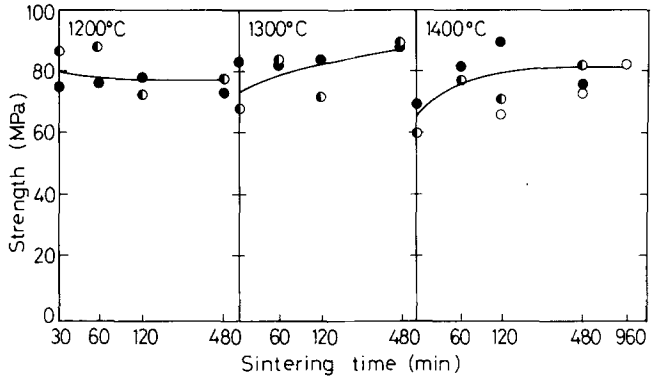

Figure 8 Variation of strength with sintering temperature, time and MgO concentration.

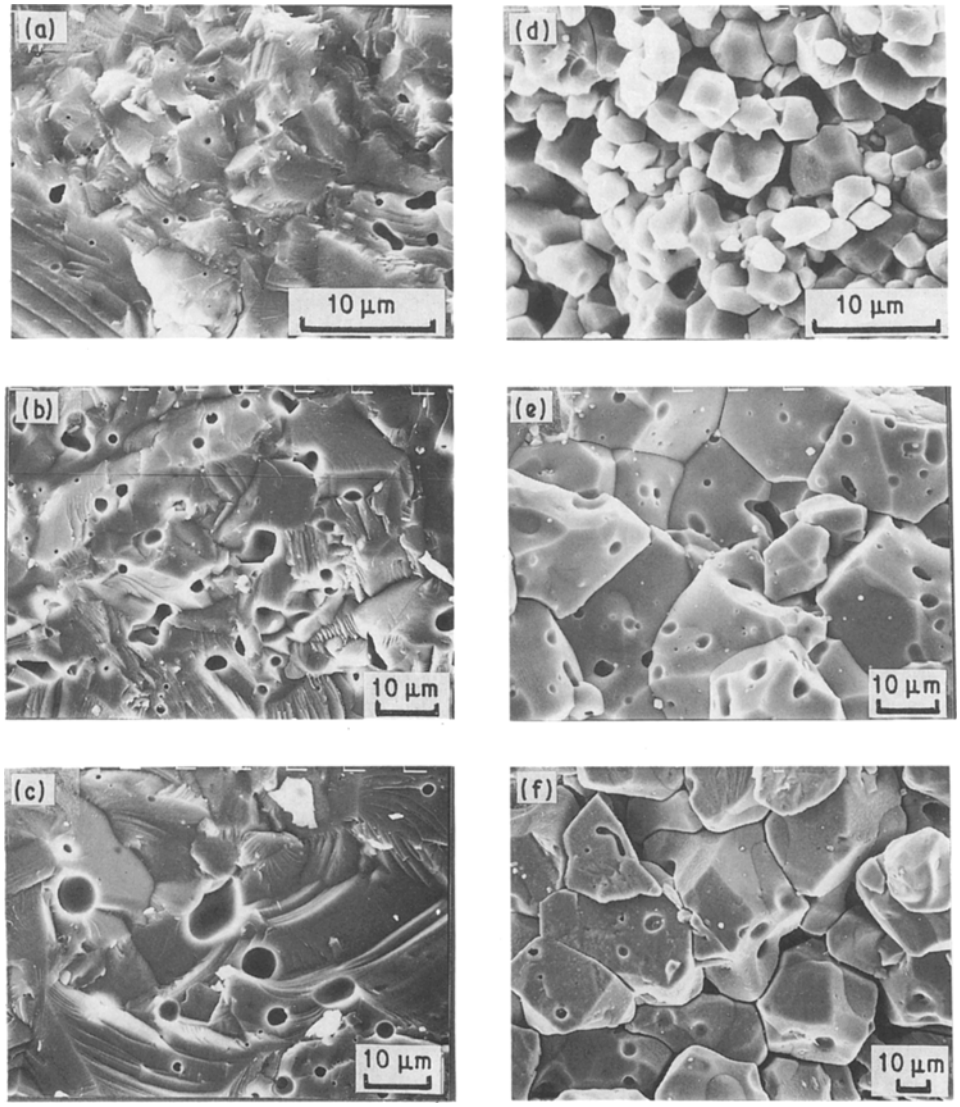

Figure 9 Scanning electron micrographs of fracture surfaces of $Sr_{0.5}Zr_2(PO_4)_3$ sintered with 1 wt % MgO at 1200° C; (a), (d) 30 min, (b), (e) 8 h, (c), (f) 1400° C for 8 h. (d) to (f) After etching.

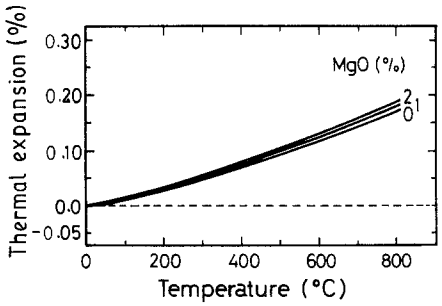

Figure 10 Thermal expansion curves of $Sr_{0.5}Zr_2(PO_4)_3$ ceramics.

an amorphous phase without any secondary phase, e.g. ZrP_2O_7 which was formed as a transient intermediate phase in the solid-state reaction method.

Fig. 6 shows the influence of calcination on densification. The green density increased with increasing calcination temperature. The bulk density of sintered ceramics also increased with increasing calcination temperature up to 1100° C, but it decreased at 1200° C. Therefore, the powder calcined at 1100° C for 1 h was chosen for subsequent runs.

Figs 7 and 8 show the variation of density and strength with sintering temperature, time and MgO concentration. The higher density was obtained with the addition of less MgO for a shorter time at lower temperature, compared to the sintering of the solid-state reaction powder. Further, the pure $Sr_{0.5}Zr_2(PO_4)_3$ powder could be densified to the relative density of 93% by sintering at 1400° C for 16 h. The strength of dense ceramics also increased to about 80 MPa, and did not change much even if the sintering was prolonged.

Fig. 9 shows the typical microstructures. As shown in Figs 9a to c, the fracture surfaces had some pores in a uniform matrix, which were similar to those of samples sintered from the solid-state reaction powder. However, as shown in Figs 9d to f, the grains in the sol–gel samples were in close contact with each other and it seemed that there was no intergranular phase, because the amount of MgO was very small. The grains grew larger with sintering time.

Fig. 10 shows the typical thermal expansion curves. Owing to the small amount of MgO, the ceramics obtained had a low linear thermal expansion coefficient of $2.4 \times 10^{-6}\,°C^{-1}$ which was near the average of the crystal.

3.2. Synthesis of $Sr_{0.5(1-x)}Nb_xZr_{2-x}(PO_4)_3$ ceramic

3.2.1. Thermal expansion of $Sr_{0.5(1-x)}Nb_xZr_{2-x}(PO_4)_3$ crystal lattice

The thermal expansion coefficient of $Sr_{0.5}Zr_2(PO_4)_3$ ceramic could never have a value below $2.1 \times 10^{-6}\,°C^{-1}$ which is the average of the crystal. Furthermore, the value of the sintered ceramics would increase because MgO was added. Therefore, in order to lower the thermal expansion, the amount of interstitial Sr^{2+} ion, which mainly contributed to the total expansion, was decreased by substituting Nb^{5+} for Zr^{4+}, as in the case of $Na_{1-x}Nb_xZr_{2-x}(PO_4)_3$ [7].

Fig. 11 shows the lattice parameters of $Sr_{0.5(1-x)}Nb_xZr_{2-x}(PO_4)_3$ plotted against temperature. Fig. 12 shows the variation of thermal expansion coefficient with x. The thermal expansion of the c-axis was almost independent of x. On the other hand, the thermal expansion of the a-axis decreased with increasing x, that is, with decreasing strontium content, and began to contract at $x \geqslant 0.5$. Consequently, the average thermal expansion coefficient became near to zero at $x = 0.5$, and then the thermal expansion anisotropy increased to some extent. However, this anisotropy was very small compared to $KZr_2(PO_4)_3$ [11], $Na_{1-x}Nb_xZr_{2-x}(PO_4)_3$ [7] or other compounds in the $NaZr_2(PO_4)_3$-type structure. Therefore, synthesis of the near-zero expansion ceramic with low thermal expansion anisotropy was attempted from $Sr_{0.25}Nb_{0.5}Zr_{1.5}(PO_4)_3$.

3.2.2. Synthesis of $Sr_{0.25}Nb_{0.5}Zr_{1.5}(PO_4)_3$ ceramic

$Sr_{0.25}Nb_{0.5}Zr_{1.5}(PO_4)_3$ powder was also densified by the addition of MgO. Fig. 13 shows the densification curves and the strength of the sintered ceramics. The results were similar to those for $Sr_{0.5}Zr_2(PO_4)_3$ ceramics. In this case, however, as niobium could decrease the melting point of the glass phase formed during sintering, the optimum amount of MgO was 3 wt %,

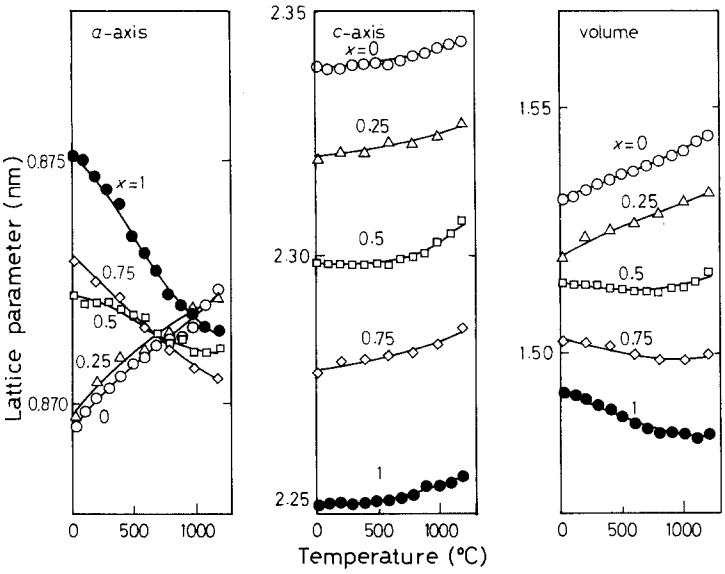

Figure 11 Lattice parameters of $Sr_{0.5(1-x)}Nb_xZr_{2-x}(PO_4)_3$ plotted against temperature.

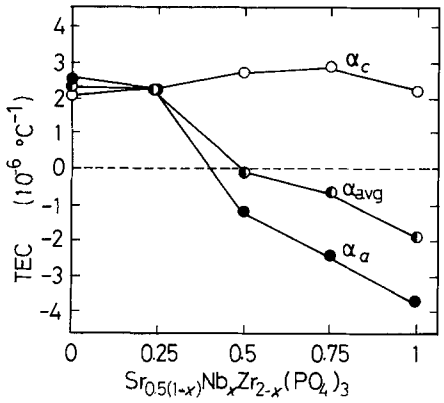

Figure 12 Thermal expansion coefficients of $Sr_{0.5(1-x)}Nb_xZr_{2-x}(PO_4)_3$ plotted against x.

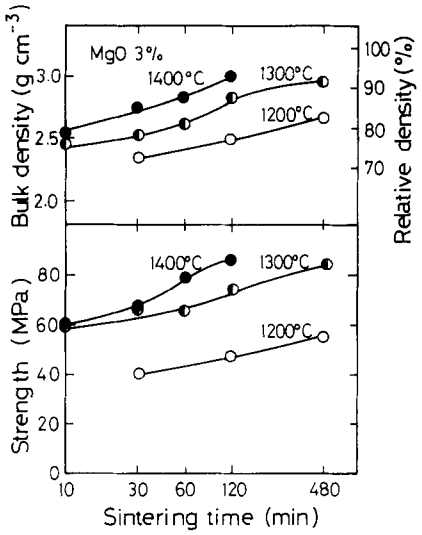

Figure 13 Variation of density and strength of $Sr_{0.25}Nb_{0.5}Zr_{1.5}(PO_4)_3$ ceramics with sintering temperature and time.

that is less than the 5 wt % needed in the case of $Sr_{0.5}Zr_2(PO_4)_3$.

Fig. 14 shows the typical microstructures. The fracture surfaces consisted of relatively large amounts of a glass phase and large pores. The grains were more rectangular in shape as shown in Figs 14d to f compared with the fracture surfaces of $Sr_{0.5}Zr_2(PO_4)_3$ in which the grains were roundish, as shown in Fig. 3. In addition, no microcracks could be found even in samples with grains over 30 μm.

Fig. 15 shows the thermal expansion curves. A sample without MgO had a slightly negative expansion curve, which could be expected from the average

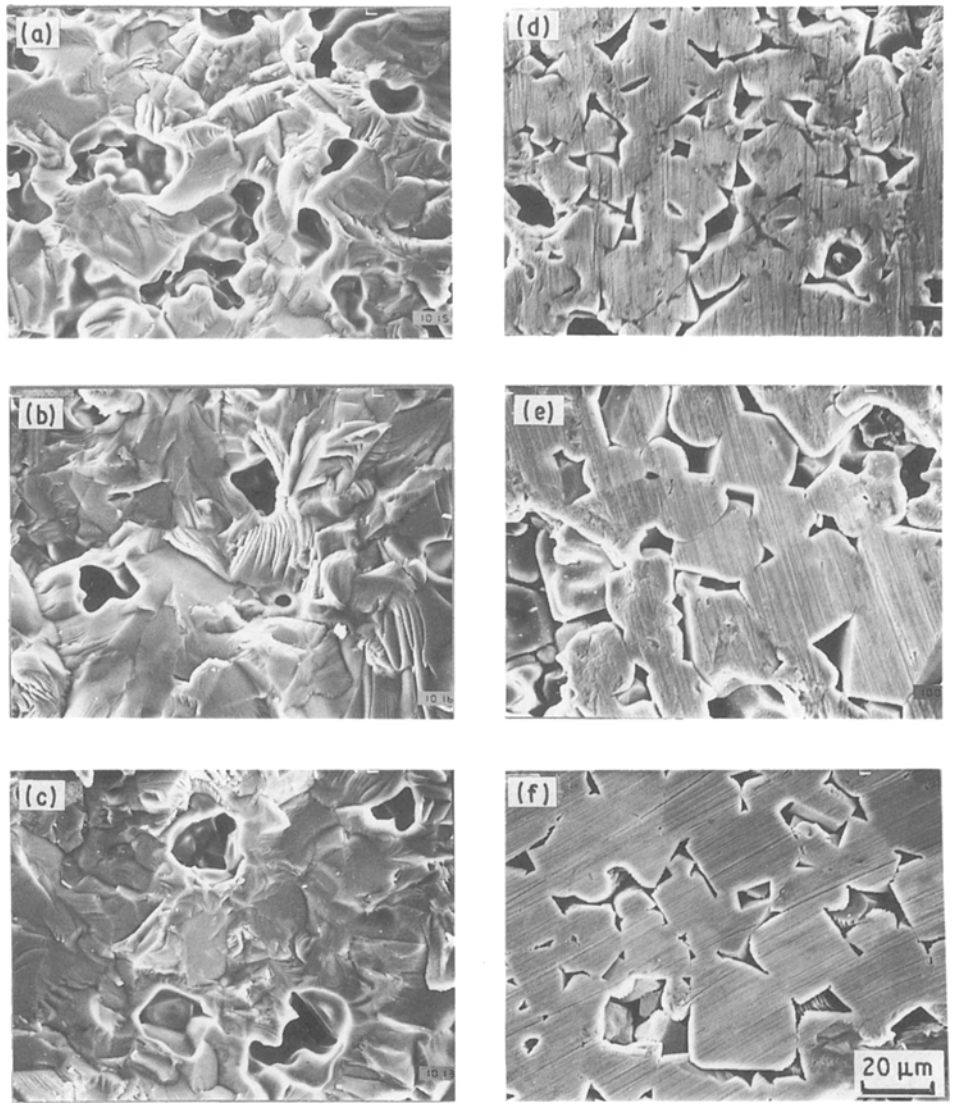

Figure 14 Scanning electron micrographs of fracture surfaces of $Sr_{0.25}Nb_{0.5}Zr_{1.5}(PO_4)_3$ sintered with 3 wt % MgO at 1300° C: (a), (d) for 2 h, (b), (e) 8 h, and (c), (f) 1400° C for 2 h. (d) to (f) After etching.

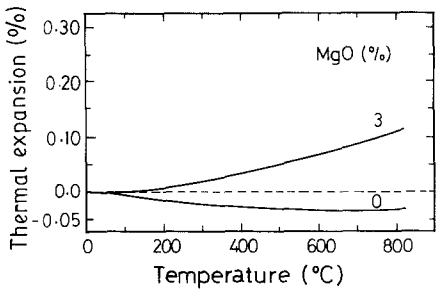

Figure 15 Thermal expansion curves of $Sr_{0.25}Nb_{0.5}Zr_{1.5}(PO_4)_3$ ceramics.

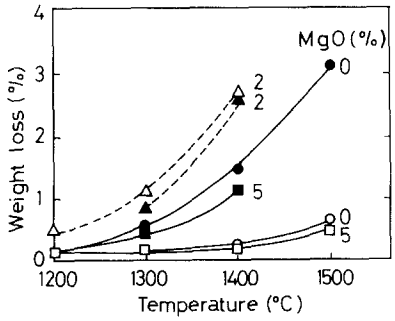

Figure 16 Weight loss of (○, □) $Sr_{0.5}Zr_2(PO_4)_3$, (●, ■) $Sr_{0.25}Nb_{0.5}Zr_{1.5}(PO_4)_3$, (△) $KZr_2(PO_4)_3$ and (▲) $NbZr(PO_4)_3$ ceramics.

of the crystal. The thermal expansion curve of the sintered ceramic became larger due to MgO addition, but it still had a very low linear thermal expansion coefficient of about $1.5 \times 10^{-6}\,°C^{-1}$.

Fig. 16 shows the weight loss of the $NaZr_2(PO_4)_3$-type ceramics. It was obvious that the ceramics in the $Sr_{0.5}Zr_2(PO_4)_3$ system presented a better stability against decomposition at high temperatures compared to $KZr_2(PO_4)_3$ [11] and $NbZr(PO_4)_3$ [7].

4. Conclusion

Dense, strong and low thermal expansion ceramics with a very low thermal expansion anisotropy were synthesized from $Sr_{0.5}Zr_2(PO_4)_3$. The densification was accelerated by adding MgO which formed a liquid phase during sintering. Consequently, the linear thermal expansion coefficient increased. By using a reactive fine powder prepared by the sol–gel method, a dense ceramic with a relative density up to 97% was obtained by sintering at 1200° C with 1 wt % MgO. The ceramic showed a linear thermal expansion coefficient of $2.4 \times 10^{-6}\,°C^{-1}$.

The $Sr_{0.5(1-x)}Nb_xZr_{2-x}(PO_4)_3$ system substituted with Nb^{5+} for Zr^{4+} and $1/2Sr^{2+}$ pairs was also investigated. The thermal expansion of the *a*-axis of the crystal decreased with x, becoming negative at $x \simeq 0.5$, while that of the *c*-axis changed little. The average thermal expansion coefficient decreased with x, becoming near zero at $x = 0.5$. The anisotropy, however, increased to some extent. The dense ceramic of $Sr_{0.25}Nb_{0.5}Zr_{1.5}(PO_4)_3$ presented a very low linear thermal expansion coefficient of about $1.5 \times 10^{-6}\,°C^{-1}$.

All ceramics in the system had a strength of about 80 MPa, which was not reduced even in the coarse-grained polycrystalline ceramics developed by prolonged sintering, because the very low thermal expansion anisotropy of the crystal did not produce any microcracks. These also decomposed little, even at 1500° C, although the substitution of niobium can somewhat lower the stability.

References

1. R. ROY, D. K. AGRAWAL, J. ALAMO and R. A. ROY, *Mater. Res. Bull.* **19** (1984) 471.
2. J. ALAMO and R. ROY, *J. Amer. Ceram. Soc.* **67** (1984) C-78.
3. G. E. LENAIN, H. A. McKINSTRY, S. Y. LIMAYE and A. WOODWARD, *Mater. Res. Bull.* **19** (1984) 1451.
4. D. K. AGRAWAL and V. S. STUBICAN, *ibid.* **20** (1985) 99.
5. D. K. AGRAWAL and R. ROY, *J. Mater. Sci.* **20** (1985) 4617.
6. T. OTA and I. YAMAI, *J. Amer. Ceram. Soc.* **69** (1986) 1.
7. I. YAMAI, T. OTA and P. JIN, *J. Ceram. Soc. Jpn* **96** (1988) 1019.
8. S. Y. LIMAYE, D. K. AGRAWAL and H. A. McKINSTRY, *J. Amer. Ceram. Soc.* **70** (1987) C-232.
9. C. DELMAS, R. OLAZCUAGA, G. LE FLEM and P. HAGENMULLER, *Mater. Res. Bull.* **16** (1981) 285.
10. J. ALAMO and R. ROY, *J. Mater. Sci.* **21** (1986) 444.
11. T. OTA and I. YAMAI, *J. Ceram. Soc. Jpn* **95** (1987) 531.
12. J. A. KUSZYK and R. C. BRADT, *J. Amer. Ceram. Soc.* **61** (1978) 478.
13. J. J. CLEAVELAND and R. C. BRADT, *ibid.* **61** (1978) 478.
14. I. YAMAI and T. OTA, *ibid.* **68** (1985) 273.
15. "Phase Diagrams for Ceramists" (The American Ceramic Society) Figs 703, 4490 and 5325–5327.

Received 21 September 1988
and accepted 24 February 1989